Chemical Engineering Journal 144 (2008) 96–102

Contents lists available at ScienceDirect

Chemical Engineering Journal

journal homepage: www.elsevier.com/locate/cej

Activity of different zeolite-supported Ni catalysts for methane reforming with carbon dioxide

Apanee Luengnaruemitchai*, Athiya Kaengsilalai

The Petroleum and Petrochemical College, Chulalongkorn University, Soi Chula 12, Phyathai Road, Bangkok 10330, Thailand

ARTICLE INFO

Article history:
Received 21 September 2007
Received in revised form 13 May 2008
Accepted 13 May 2008

Keywords:
CH_4
CO_2 reforming
Ni
Zeolite
Carbon deposition

ABSTRACT

The catalytic performance of Ni based on various types of zeolites (zeolite A, zeolite X, zeolite Y, and ZSM-5) prepared by incipient wetness impregnation has been investigated for the catalytic carbon dioxide reforming of methane into synthesis gas at 700 °C, at atmospheric pressure, and at a CH_4/CO_2 ratio of 1. It was found that Ni/zeolite Y showed better catalytic performance than the other types of studied zeolites. In addition, the stability of the Ni/zeolite Y was greatly superior to that of the other catalysts. A weight of Ni loading at 7 wt.% showed the best catalytic activity on each zeolite support; however, the 7% Ni catalysts produced a higher amount of coke than that of two other Ni loadings, 3 and 5%.

1. Introduction

The CO_2 reforming of CH_4 has become interesting for industries since it converts the two cheapest and most abundant greenhouse gases (CH_4 and CO_2) to useful synthesis gas (H_2/CO). A major problem encountered in this process is carbon deposition on the surface, leading to deactivation and causing the blockage of reactor tubes. Besides coke formation, sintering of the metal particles can also account for the loss of catalytic activity. Although numerous supported catalysts in Group VIII metals, particularly Rh and Ru, are suitable for the CO_2 reforming of CH_4 due to less carbon deposition [1,2], the high cost of these two metals still limits their commercial acceptance. The Ni catalyst is used industrially for both steam reforming and dry reforming reactions because of its fast turnover rates, availability and low cost; although it is more sensitive to coke formation than other noble metals [3] since it can catalyze carbon formation via methane decomposition ($CH_4 \leftrightarrow C + 2H_2$, $\Delta H_{298} = 75$ kJ/mol) and the Boudouard reaction ($2CO \leftrightarrow C + CO_2$, $\Delta H_{298} = -172$ kJ/mol).

Apart from the metal, the catalyst support plays an important role on coke resistance of the metal particles and may even participate in the catalytic reactivity. Among the materials used as a support for this reaction such as SiO_2 [4], MgO [5,6], Perovskite [7], CeO_2 [8], and γ-Al_2O_3 [9], alumina is usually used as a catalyst support. However, it is unstable at high temperatures because of the thermal deterioration of the Al_2O_3 support as well as the phase transformation into α-Al_2O_3 [10]. This means that the development of the catalyst support is usually the subject of investigation in order to enhance both the catalytic activity and the stability of the Ni-based catalysts. The effect of promoter, such as Ag, La [11], Mg, Mn, K, and Ca [12], was investigated for improving the stability of the Ni catalysts for CH_4 reforming.

Zeolite is an attractive support for the CO_2 reforming of CH_4 since it is known to have a well-defined structure, high surface area, high thermal stability, and high affinity for CO_2, which is expected to enhance both the catalytic activity and the stability. The use of Ni supported on zeolites in the dry reforming of CH_4 has been studied by Chang et al. [13]. They found that Ni supported on ZSM-5 zeolite showed high activity with high resistance to coke formation for the CO_2 reforming of CH_4. This is due to its large specific surface area (340 m^2/g) and its well-defined structure, which allows for a high dispersion of active metal on the surface [14]. Jeong et al. [12] investigated a series of Ni/HY catalysts modified by Mg, Mn, K, and Ca. It was observed that the Ni–Mg/HY catalyst showed the highest carbon resistance and the most stable catalytic performance. Additionally, Ni/H-mordenite [15], KNiCa/ZSM5 [16], Ni/USY-type zeolite [17,18] catalysts were also investigated for this reaction and their high activity and stability have been reported. Therefore, it is more practical to study an improved catalyst comprising Ni and zeolite as a catalyst support.

Based on our earlier work, the potential of zeolites clinoptiolite [19], KH [20], and KL [21], for the CO_2 reforming of CH_4 were reported as good candidates based on their high activity and stability compared to an Al_2O_3 support. The effects of Ni loading and

* Corresponding author. Tel.: +66 2 218 4148; fax: +66 2 215 4459.
E-mail address: apanee.l@chula.ac.th (A. Luengnaruemitchai).

1385-8947/$ – see front matter © 2008 Elsevier B.V. All rights reserved.
doi:10.1016/j.cej.2008.05.023

promoter on the catalytic behavior were investigated and stability testing was also done. Accordingly, the catalytic performance of a series of zeolite-supported Ni catalysts was investigated for the dry reforming of CH_4. In this present work, zeolite A, zeolite X, zeolite Y and ZSM5 were used as the support due to their high thermal stability [22,23]. The aim of the present contribution was to evaluate the activity and stability of a series of catalysts for the dry reforming of CH_4. The structural properties and the coke formation of these catalysts have been investigated extensively.

2. Experimental

2.1. Catalyst preparation

Zeolite A (BET area 26.77 m^2/g), zeolite X (BET area 426.70 m^2/g), and zeolite Y (BET area 606.15 m^2/g) were obtained from IFP (France) in sodium form with Si/Al = 1.0, 1.349, and 2.833, respectively. ZSM-5 (BET area 291.59 m^2/g) was obtained from UOP (USA) with Si/Al = 398. A series of Ni-based catalysts was prepared with different total Ni contents (3, 5, and 7 wt.%). The catalysts were prepared by an incipient wetness impregnation using $Ni(NO_3)_2{\cdot}6H_2O$ (Merck) as the metal precursors. After impregnation, the catalyst samples were dried overnight at 110 °C and were subsequently calcined in air at 500 °C for 5 h.

2.2. Catalyst characterization

The crystallinity of the prepared catalysts was identified using powder X-ray diffraction (XRD) on a Rigaku X-ray diffractometer system equipped with a RINT 200 wide-angle goniometer using Ni-filtered Cu Kα radiation with a generator voltage and current of 40 kV and 30 mA, respectively. A scan speed of 5° (2θ min^{-1}) with a scan step of 0.002° (2θ) was applied during a continuous run in the 5–60° (2θ) range. Phase identification was carried out using the reference database (JCPDS-files) supplied with the equipment. The Brunauer–Emmett–Teller (BET) method, using a Quantachrome Corporation Autosorb, was used to determine the total surface area of the prepared catalysts by N_2 adsorption/desorption at −196 °C. Temperature-programmed reduction (TPR) was carried out on a TPDRO 1100 to monitor the reduction of the metal oxide. The sample was first pretreated in a flow of He at 200 °C and then reduced under a flow of 5.32% H_2/N_2 mixture (20 ml/min). The sample was heated from 60 to 900 °C with a heating rate of 10 °C/min. After reaction at 700 °C for 5 h, temperature-programmed oxidation (TPO) was performed to study the reactivity of the carbon species by oxidizing the sample under a flow of air while the temperature was increased from room temperature to 800 °C linearly with time with a heating rate of 10 °C/min.

2.3. Catalytic performance

The experiments were performed in a fixed-bed reactor, with an inner diameter of 6 mm, imbedded in an insulated electric furnace equipped with a temperature programmable controller. A K-type thermocouple was inserted into the catalyst bed to measure and control the bed temperature. The reactant gas stream consisted of CO_2 and CH_4 with a molar ratio of 1:1 at a total flow rate of 100 ml/min (GHSV = 30,000 $cm^3/h\,g\,cat$). A fresh 0.2 g catalyst sample (80–120 mesh) was packed into the reactor and reduced in flowing hydrogen at 600 °C for 1 h and then was purged with flowing helium at the reaction temperature for 30 min. The catalytic activity was studied at 700 °C for 5 h. The gas compositions of the reactants and products were analyzed by a Hewlett Packard 5890 Series II equipped with a Carbosphere packed column and a thermal conductivity detector. The conversions of CH_4 and CO_2 and the selectivity of H_2 and CO are defined as follows:

$$X_{CH_4} = \frac{[CH_4]_{in} - [CH_4]_{out}}{[CH_4]_{in}} \times 100$$

$$X_{CO_2} = \frac{[CO_2]_{in} - [CO_2]_{out}}{[CO_2]_{in}} \times 100$$

$$S_{H_2} = \frac{1}{2}\frac{[H_2]_{out}}{[CH_4]_{in} - [CH_4]_{out}} \times 100$$

$$S_{CO} = \frac{[CO]_{out}}{[CH_4]_{in} - [CH_4]_{out} + [CO_2]_{in} - [CO_2]_{out}} \times 100$$

where $[CH_4]_{in}$ and $[CO_2]_{in}$ are the flow rates of the introduced reactants and $[CH_4]_{out}$, $[CO_2]_{out}$, $[H_2]_{out}$, and $[CO]_{out}$ are the flow rates of the corresponding compositions in the effluents. No by-products were observed in this experiment.

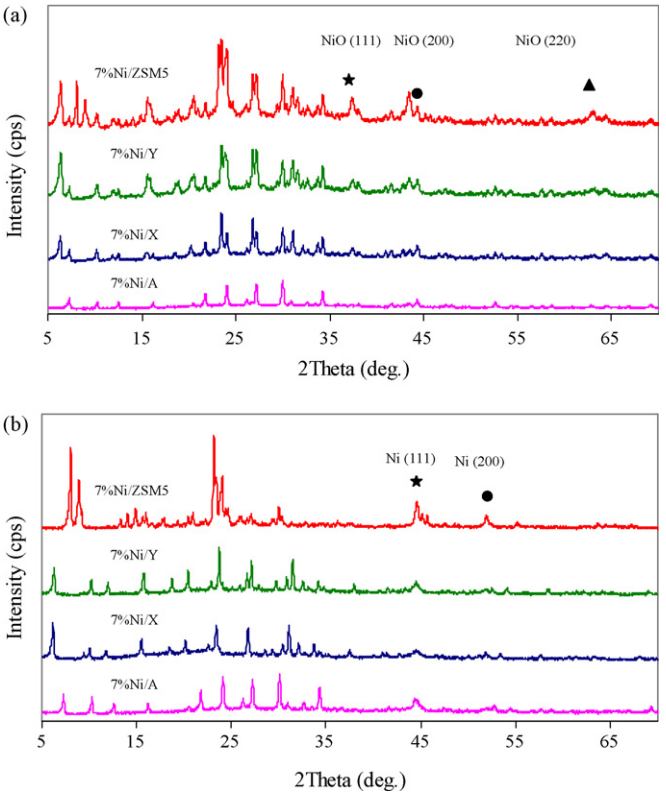

Fig. 1. X-ray diffraction patterns of 7%Ni/zeolite catalysts: (a) calcined catalyst and (b) reduced catalyst.

3. Results and discussion

3.1. Catalyst characterization

Typical XRD patterns for all fresh and reduced Ni supported on zeolite catalysts were recorded and illustrated as shown in Fig. 1. The effect of Ni loading was estimated from the XRD spectrum (not shown here) and it was found that the crystallinity of the zeolite decreased slightly upon Ni incorporation, in agreement with the results reported by Kiessling et al. [24]. The XRD profiles of Ni/zeolite catalysts were typical of crystalline LTA, FAU and ZSM5 materials. Diffraction peaks of NiO at 2θ = 37.2°, 43.2°, and 63° are clearly detected for all samples. The particle sizes of NiO and Ni were calculated from line broadening analysis and the results are

Table 1
Crystallite sizes of calcined and reduced Ni/zeolite catalysts

Catalyst	NiO(1 1 1) (nm)	NiO(2 0 0) (nm)	NiO(2 2 0) (nm)	Ni(1 1 1) (nm)	Ni(2 0 0) (nm)
Calcined 7% Ni/zeolite A	18.05	19.01	14.17		
Reduced 7% Ni/zeolite A				–	–
Calcined 7% Ni/zeolite X	18.65	19.01	20.73		
Reduced 7% Ni/zeolite X				54.39	55.96
Calcined 7% Ni/zeolite Y	9.32	19.01	20.72		
Reduced 7% Ni zeolite Y				54.39	65.49
Calcined 7% Ni/ZSM-5	7.43	12.59	20.72		
Reduced7% Ni/ZSM-5				27.28	55.98

tabulated in Table 1. It should be noted that the sizes of the Ni particles in the Ni/ZSM5 were the smallest, indicating that Ni sizes were highly dispersed on the surface of the catalyst. On the other hand, no diffraction peaks of metallic Ni species were observed in the XRD patterns of the reduced Ni/zeolite A catalyst at $2\theta = 44.5^\circ$ and 51.8°, suggesting that NiO was not completely reduced at this temperature.

The observation of several peaks in the TPR profiles of 7% Ni/zeolite catalysts, shown in Fig. 2, indicates the presence of different reduction sites. According to Afzal et al. [25], the reduction peaks at lower temperature are attributed to the reduction of the Ni^{2+} localized in the supercage and/or sodalite cavities, whereas that at high temperatures are attributed to the reduction of the Ni^{2+} localized in hexagonal cavities. For Ni/ZSM5, one clearly resolved maximum is observed at 420 °C and a shoulder at ~320 °C, which corresponds to the reduction of NiO particles without or with very low interaction with the support [26,27] or the reduction of Ni^{2+} from NiO formed particles on the outer surface of the zeolite crystals [28]. The value of the maximum of TPR peak for the Ni/ZSM5 at 420 °C is significantly higher as compared to that of other samples. This can be related to the difference in the size of the NiO particles or might be the reduction of NiO on the outer surface of the zeolite structure. A reduction of peak area at this low temperature range would be consistent with a slight decrease in the Ni content present on the catalyst surface.

Ni/zeolites X and Y show two maxima at ~420 and ~650 °C; however, there is a high temperature peak at ~720 °C in the profile of Ni/zeolite X. The peak at the lower temperature can be assigned to the reduction of NiO with very low interaction with the support and the peak at the higher temperature region is the reduction of NiO particles with high interaction with the support [29]. It is more likely that the Ni/zeolite Y would have a larger amount of the Ni species located on the outer zeolite surface than the Ni/zeolite X. Similar features were observed in the profile of Ni/zeolite Y prepared by an ion-exchange with small peaks at ~460 and 650 °C, whereas the main peak was observed at 840 °C [30]. The latter is attributed to the reduction of Ni^{2+} in hexagonal prisms. The higher intensity of the low-temperature peak in the present work suggests that the incorporation of Ni prepared by an impregnation would lead to a higher amount of Ni^{2+} in the supercages and the absence of peaks at high temperatures indicates that there is no Ni^{2+} in the hexagonal prisms.

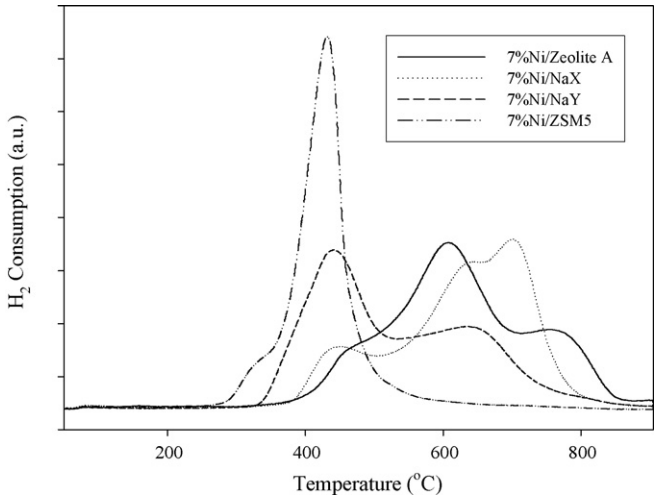

Fig. 2. TPR profiles of 7% Ni/zeolite catalysts.

For the Ni/zeolite A catalyst, a few literature data are available on the reduction of metal cations on A zeolite. The maximum in the hydrogen consumption is located at ~600 °C, which agrees well with Afzal et al. They found that the TPR of Ni/zeolite A is centered at temperature of 625 °C, meaning that the metal cations are located in six-rings and are more difficult to reduce. Additionally, two shoulders, at ~450 and 780 °C, are observed in this present work. The latter might be associated with the reduction of the Ni species located on the hexagonal prism [31], which agrees well with the XRD result of the reduced Ni/zeolite A.

3.2. Effect of Ni loading on the performance of Ni/zeolite catalyst

3.2.1. Ni/zeolite A

Catalytic activity was carried out over a series of Ni/zeolite A with Ni loadings of 3, 5, and 7 wt.% at 700 °C for 5 h. The results of CH_4 and CO_2 conversions of the samples are shown in Fig. 3(a and b). As depicted, both the CH_4 conversion and CO_2 conversion increase with the rise of Ni loading. It was revealed that 7% Ni supported on zeolite A can give very high activity on both CH_4 and CO_2 conversions (~70–80%); however, the conversions decreased with increasing time-on-stream. The initial CH_4 conversion was estimated at 70%, but it drastically decreased to 15% after 5 h. However, for 3% and 5% Ni/zeolite A, the reaction was ended after 1 and 3 h, respectively; neither CH_4 nor CO_2 was converted to products. Their catalytic activity showed much lower activity than 7% Ni/zeolite A.

For H_2 selectivity, as shown in Fig. 3(c), the trend of the CH_4 and CO_2 conversions was also followed. The 7% Ni/zeolite A initially provided H_2 selectivity estimated at 55%, then eventually decreased along with time-on-stream due to the depression of CH_4 conversion (Fig. 3(a)). However, the CO selectivity on 7% Ni/zeolite A was increased along testing time, which was contrary to the trend compared to others.

3.2.2. Ni/zeolite X

Fig. 4 presents the catalytic performance of a series of Ni/zeolite X with Ni loadings of 3, 5, and 7% at 700 °C for 5 h. The catalytic activity on the 7% Ni/zeolite X catalysts also showed the highest activity of the catalysts and was quite constant along testing time. In addition, the 5% Ni/zeolite X revealed a similar trend as the 7% Ni/zeolite X, while the activity on the 3% Ni/zeolite X

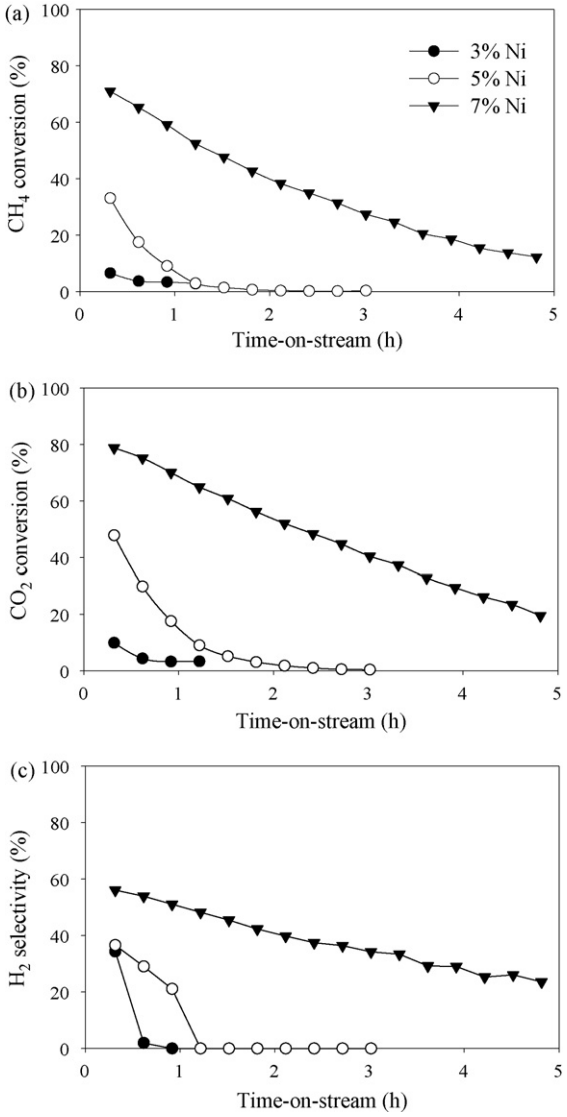

Fig. 3. Effect of Ni loading over Ni/zeolite A on the catalytic activity in the CO_2 reforming of CH_4 at 700 °C: (a) CH_4 conversion, (b) CO_2 conversion, and (c) H_2 selectivity.

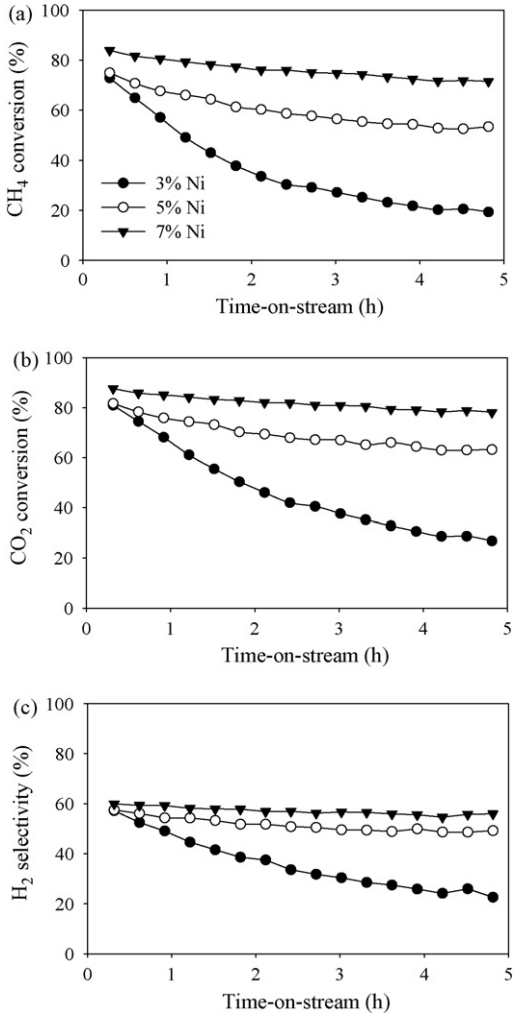

Fig. 4. Effect of Ni loading over Ni/zeolite X on the catalytic activity in the CO_2 reforming of CH_4 at 700 °C: (a) CH_4 conversion, (b) CO_2 conversion, and (c) H_2 selectivity.

catalyst dramatically decreased with increasing time-on-stream. The H_2 selectivity, as presented in Fig. 4(c), also showed a similar trend as the CH_4 and CO_2 conversions. 7% Ni/zeolite X exhibited about 60% H_2 selectivity; however, in comparison, Ni/zeolite X exhibited a higher H_2 selectivity than that of Ni/zeolite A, especially at the initial time.

3.2.3. Ni/zeolite Y

The results of CH_4 and CO_2 conversions with time-on-stream over Ni/zeolite Y catalysts with various Ni content (3, 5, and 7 wt.%) are shown in Fig. 5(a and b). The 5% and 7% Ni/zeolite Y revealed similar activity and it was maintained along the time-on-stream. No significant difference in both the conversions of 5% and of 7% Ni supported on zeolite Y catalysts was observed, while the conversion with 3% Ni/zeolite Y was decreased with increasing time-on-stream. The 7% Ni supported on zeolite Y gave ~92% CH_4 conversion after 5 h. However, the conversions of CH_4 and CO_2 with 5% Ni/zeolite Y in this work were much higher than that of 5% Ni/HY reported by Jeong et al. [12], which exhibited about 35% and 39% conversions of CH_4 and CO_2, respectively, after 1 h of reaction. It was found that conversion and product yield were increased with increasing Ni loading up to 13 wt.% which exhibited 93% CH_4 conversion at 700 °C and a mole ratio of $CH_4/CO_2 = 1$.

For H_2 selectivity, as illustrated in Fig. 5(c), the trends of CH_4 and CO_2 conversion was also followed. The 5% and 7% Ni/zeolite Y catalysts can provide a H_2 selectivity of ~65%. However, the catalytic performance on Ni/zeolite Y had a better activity trend than that with Ni/zeolite A and Ni/zeolite X catalysts, especially in terms of thermal stability of the studied catalysts.

3.2.4. Ni/ZSM-5

The catalytic activity of a series of Ni/ZSM-5 catalysts with Ni loadings of 3%, 5%, and 7% at 700 °C for 5 h was also investigated. The results of CH_4 and CO_2 conversions on ZSM5-supported Ni catalysts are shown in Fig. 6. The 5% Ni/ZSM-5 catalyst showed different trends compared to 3% and 7% Ni/ZSM-5 catalysts. Its conversions were quite constant along testing time while the 3% and 7% Ni/ZSM-5 were slightly depressed with increasing time-on-stream. This is in accordance with the 5.3% Ni/ZSI reported by Chang et al. [13]. It exhibited 78% CH_4 and 78% CO_2 conversions at 700 °C and coke formation was greatly increased at higher Ni loadings. It was concluded that zeolite-supported Ni catalysts without

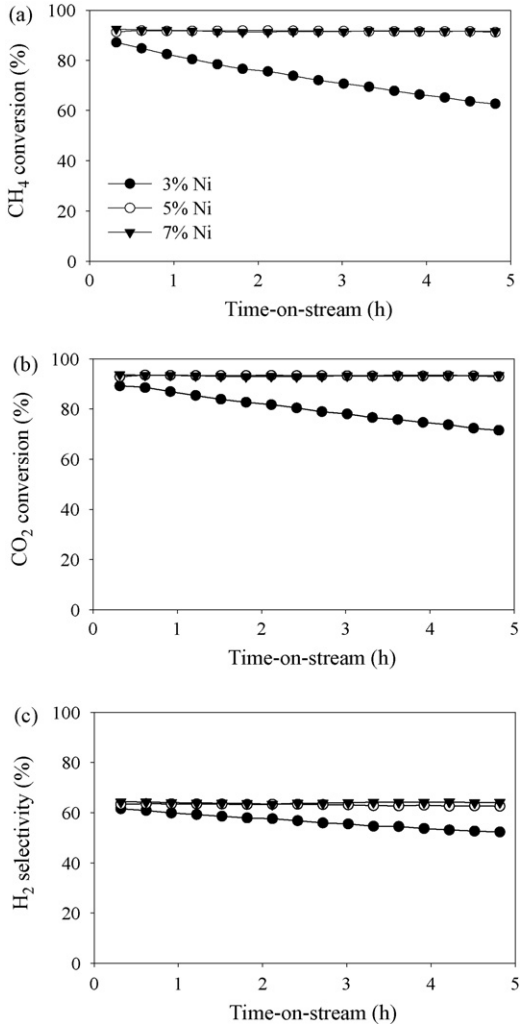

Fig. 5. Effect of Ni loading over Ni/zeolite Y on the catalytic activity in the CO_2 reforming of CH_4 at 700 °C: (a) CH_4 conversion, (b) CO_2 conversion, and (c) H_2 selectivity.

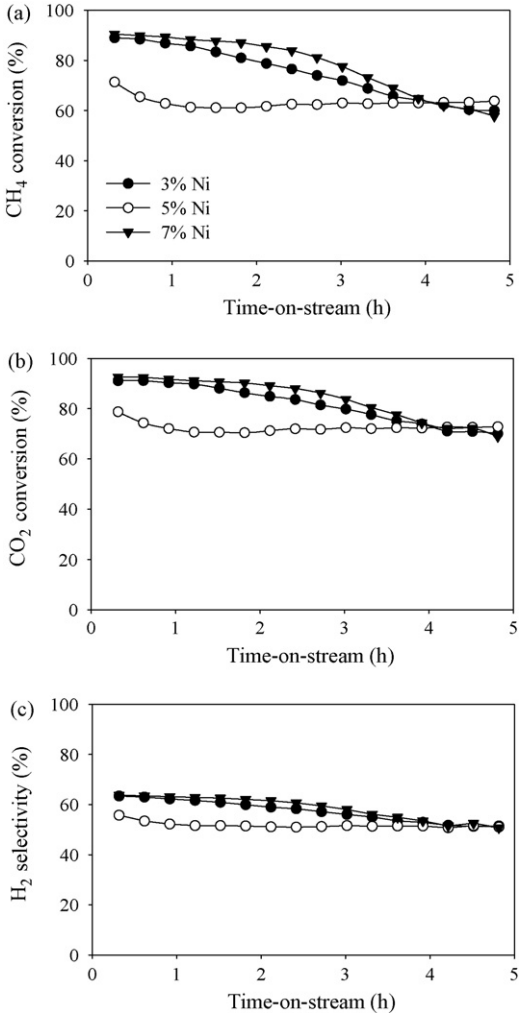

Fig. 6. Effect of Ni loading over Ni/ZSM-5 on the catalytic activity in the CO_2 reforming of CH_4 at 700 °C: (a) CH_4 conversion, (b) CO_2 conversion, and (c) H_2 selectivity.

alkaline promoters are readily deactivated due to the high reactivity toward methane [16]. The KNiCa/ZSI showed high activity and high resistance against coke formation, whereas the Ni/ZSI exhibited high activity (~92% CO_2 conversion) at initial period of reaction and its activity rapidly decreased within 30 h. The zeolite support was a highly siliceous ZSM5 (UOP S-115 S_{BET} = 340 m^2/g, Si/Al > 200) mixed with alumina (19.5 wt.%). Although Rh-based catalysts are active for this reaction, the performance of 1% Rh/ZSM-5 catalyst [1], which exhibited about 28–34% CH_4 conversion, was found to be much lower compared to Ni/ZSM5 in the present study.

As shown in Fig. 6(c), the 3% and 7% Ni/ZSM-5 catalysts provided a H_2 selectivity of ~65%. However, the CO selectivity of the 5% Ni/ZSM-5 catalyst was increased with increasing time-on-stream, which is contrary to the other activities. Besides, the 3% and 7% Ni/ZSM-5 catalysts provided an initial H_2 production around 80%, but was gradually depressed during the reaction process. And after 4 h, there were no significant differences in the H_2 production of all studied Ni/ZSM-5s.

3.3. Carbon deposition on spent catalysts

The most widely used technique for analysis of the reactivity of coke is the TPO technique. After the reaction, the spent samples were subjected to TPO treatment to investigate the carbon deposition of Ni/zeolite with different Ni contents. As illustrated in Fig. 7(a), the oxidation of inert carbon or graphitic carbon on Ni/zeolite Y began next to 400 °C and the peak was between 600 and 650 °C, varying with Ni content. It can be observed that the 7% Ni/zeolite Y shows a defined profile, indicating only one type of carboneous specie was found on the catalysts. While 3% Ni/zeolite Y displays an extremely weak signal, indicating a negligible carbon deposition. The CO_2 formation increased with the increase of Ni content, which is consistent with the same tendency observed in the activity experiment.

The effect of Ni loading on the Ni/zeolite catalysts for the CO_2 reforming of CH_4 showed that the activity was a function of Ni loading for all catalysts (Figs. 3–6). 7% Ni loading on the studied zeolites gave the highest activity; however, this catalyst also produced a large amount of carbon. It shows that the amount of carbon deposition increases with a Ni content increase from 3% to 7%. These findings indicate that there are many factors affecting the carbon formation. This is consistent with the literature in that, for dry reforming, the relative ease with which carbon is oxidized from the surface affects the catalytic activity more than the actual amount of carbon on the catalyst surface [32], and the whisker carbon does not necessarily lead to deactivation [33]. There are three types of carboneous species, α-C, β-C, and γ-C species exist on the Ni catalysts.

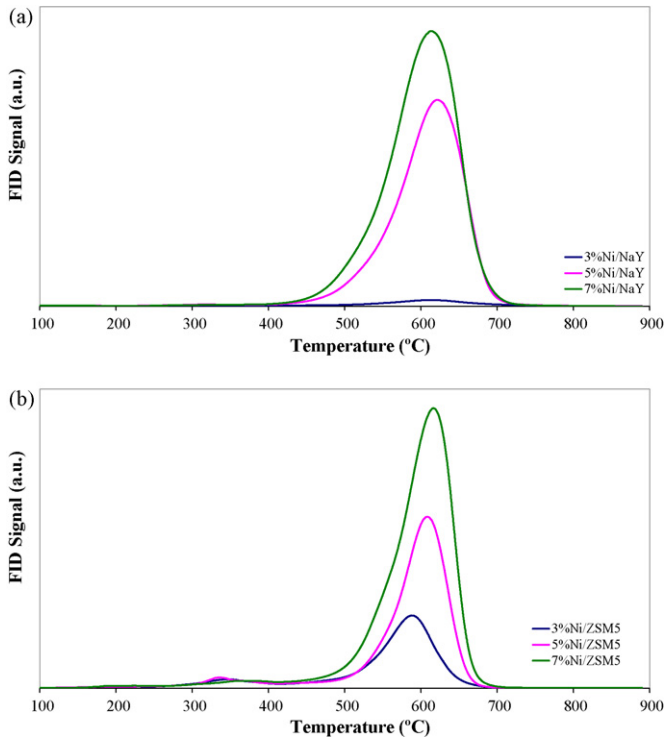

Fig. 7. Comparison of TPO profiles of (a) Ni/zeolite Y and (b) Ni/ZSM5 catalysts with various Ni loadings.

It has been reported that α-C species is suggested to be responsible for CO formation, whereas the less active species, β-C and γ-C, are causing catalyst deactivation [34].

According to the TPO curves of Ni/ZSM5 shown in Fig. 7(b), the first low temperature peak with weak intensity at ~330 °C and the second peak with high intensity at ~620 °C were clearly observed, implying at least two types of carboneous species were formed. Additionally, a similar general increase in intensity with increasing Ni loading was observed, as compared to Ni/zeolite Y. Ni/zeolite A presents three peaks at around 150, 250, and 450 °C, whereas three peaks located at 100, 350, and 450 °C are present in the TPO profile of Ni/zeolite X (not shown here). The first one is assigned to the oxidation of the poorly polymerized coke deposited on the metal particles or in its vicinity and the second is the highly polymerized coke deposited near the metal–support interphase. The last one corresponds to coke deposited on the support. The amount of coke deposited on the spent catalysts measured by TPO is given in Table 2. The largest amount of coke was formed over Ni/zeolite Y, in comparison with other catalysts. It should be noted that the amount of coke deposited on the metal is smaller than that on the support. Under the similar conditions, Ni/zeolite A and Ni/zeolite X showed much lower the coke amount than Ni/ZSM5 and Ni/zeolite Y.

Table 2
Effect of catalyst supports on the performance of Ni/zeolite catalysts in the CH_4 reforming with CO_2 after 5 h

Catalyst	CH_4 conversion (%)[a]	H_2/CO	Amount of coke (%)[b]
7% Ni/zeolite A	12.3	0.31	0.25
7% Ni/zeolite X	71.5	1.27	0.24
7% Ni/zeolite Y	91.6	1.79	6.83
7% Ni/ZSM-5	57.8	1.03	2.16

[a] T = 700 °C, pressure = 1 atm, and molar ratio of CH_4/CO_2 = 1/1.
[b] As measured by TPO.

3.4. Effect of zeolite supports

It is widely known that the catalyst support plays an important role in the conversion processes and the nature of the support greatly affects the catalytic performance due to the active surface area and acid–base property. Since this reaction involves the adsorption and dissociation of CO_2 on the surface, as CO_2 is an acid gas, the adsorption and dissociation of CO_2 on the surface may be improved with a basic support.

The initial CH_4 conversion at 700 °C over the Ni supported on a variety of zeolite supports; zeolite A, zeolite X, zeolite Y, and ZSM-5 decreases in the order: Ni/ZSM-5 > Ni/zeolite Y > Ni/zeolite X > Ni/zeolite A. Noticeably, the reduction of the Ni species in the Ni/ZSM5 (from TPR) occurred at lower temperatures than in the Ni/zeolite Y and Ni/zeolite X. According to the TPR results, it is likely that the Ni/ZSM5 would have a larger amount of the Ni species located on the outer zeolite surface or in the supercages. The Ni/ZSM5 had therefore an initial conversion comparable to supported-zeolite Y catalyst; its stability, however, was significantly worse. A reduction of peak area at this low temperature range would be consistent with a slight decrease in the Ni content present on the catalyst surface. In the case of Ni/zeolite A, a shoulder at 780 °C was observed which attributed to the reduction of the Ni species located on the hexagonal prism. This could imply that the Ni species located on the hexagonal prism, which are difficult to be reduced as mentioned previously, were not active.

Table 2 shows the comparison of CH_4 conversions and H_2/CO ratios produced after 5 h of reaction from the Ni/zeolite catalysts. The results show a clear difference in the CH_4 conversion among the supports tested; decreasing in the following order: Ni/zeolite Y > Ni/zeolite X > Ni/ZSM-5 > Ni/zeolite A. It should be noted that CH_4 conversion was consistent with the H_2/CO ratio. The prepared catalysts gave different numbers in the H_2/CO ratios after 5 h of reaction, which were higher than 1 due to faster decomposition of methane, except the Ni/zeolite A catalyst (~0.31). The result is in good agreement with our previous work [20]; Ni/KH zeolite gave a H_2/CO ratio of ~1.5 whereas Ni/γ-alumina gave a H_2/CO ratio of 0.82 under the same conditions. According to the stoichiometry of the overall reaction scheme, the CO_2 conversion is similar to or higher than that of CH_4 because the reverse water gas shift (RWGS) reaction occurs simultaneously to the CO_2 reforming of CH_4 [35]. Therefore, this reaction consumes more CO_2 and produces more CO, leading to a lower H_2/CO ratio. It can be observed that the RWGS reaction is favored over the Ni/zeolite A catalyst since the H_2/CO ratio obtained from this catalyst is much lower than those catalysts tested. Excellent results can be obtained with catalysts containing low amounts of Lewis acid sites, such as zeolite Y. The 7% Ni/zeolite Y gave the highest H_2/CO ratio equal to 1.79 and displayed the highest activity in spite of having higher carbon content; therefore, it is suggested as a suitable support for this reaction.

As clearly shown in Figs. 3–6, over the testing time of 5 h, no deactivation was observed for Ni/zeolite Y. And the deactivation rates of the prepared catalysts followed the order of: Ni/zeolite Y < Ni/zeolite X < Ni/ZSM-5 < Ni/zeolite A. The performance of the 7% Ni/zeolite Y and 7% Ni/ZSM-5 catalysts after 5 h of reaction time reached 91.6% and 57.8% of CH_4 conversion, respectively, which is much higher than that of the catalysts reported by Halliche et al. [36] and Zhang et al. [14]. Halliche et al. reported that after 6 h of reaction time the 8.7% Ni/USY (Si/Al = 4.5) and 3.5% Ni/ZSM-5 (Si/Al = 14) catalysts reached 71.2% and 54.3% of CH_4 conversion and 71.2% and 56.3% of CO_2 conversion, respectively, at 650 °C and CO_2/CH_4 = 1, while Zhang et al. found that CH_4 conversion over the Ni/ZSM-5 catalyst dramatically decreased as the time-on-stream increased. At about 5 h of reaction, it gave a CH_4 conversion of an estimated 38%.

4. Conclusions

The CO_2 reforming of CH_4 is efficiently catalyzed by zeolite-supported Ni catalysts. Lower Ni content catalysts obviously deactivated with time-on-stream. In summary, 7 wt.% Ni was considered as the optimum value for all zeolites examined. The activity towards methane conversion depended on many parameters, such as the amount of Ni and the nature of the support material. A high CH_4 conversion (91.6%) is easily achieved by 7% Ni/zeolite Y with deactivation not observed. It demonstrated greatly superior activity (both for CH_4 and for CO_2 conversions) and stability, and a higher H_2/CO ratio when compared to those of Ni supported on zeolite catalysts. Finally, it was found that zeolite Y has very good potential for being a support for Ni catalysts for the dry reforming of CH_4.

Acknowledgements

This study was financially supported by the TRF Master Research Grants, Thailand Research Fund. The authors also thank Ms. Pattarasuda Naknam for the catalyst characterizations of TPR and XRD.

References

[1] R.N. Bhat, W.M.H. Sachtler, Appl. Catal. A: Gen. 150 (1997) 279–296.
[2] V.A. Tsipouriari, A.M. Efstahiou, X.E. Verykios, Catal. Today 21 (1994) 579–587.
[3] S. Wang, G.Q.M. Lu, Appl. Catal. B: Environ. 16 (1998) 269–277.
[4] E. Kuijpers, J. Jansen, A.J. van Dillen, J.W. Geus, J. Catal. 72 (1981) 75–82.
[5] A. Parmaliana, F. Arena, F. Frusteri, S. Coluccia, L. Marchese, G. Martra, A. Chuvilin, J. Catal. 141 (1993) 34–47.
[6] O. Yamazaki, T. Nozaki, K. Omata, K. Fujimoto, Chem. Lett. 21 (1992) 1953–1954.
[7] T. Hayakawa, S. Suzuki, J. Nakamura, T. Uchijima, S. Hamakawa, K. Suzuki, T. Shishido, K. Takehira, Appl. Catal. A: Gen. 183 (1999) 273–285.
[8] K. Asami, X. Li, K. Fujimoto, Y. Koyama, A. Sakurama, N. Kometani, Y. Yonezawa, Catal. Today 84 (2003) 27–31.
[9] T. Tsuchida, Appl. Catal. A: Gen. 105 (1993) 141–149.
[10] Z. Chen, Q. Wu, J. Li, Q. Zhu, Catal. Today 30 (1996) 147–155.
[11] N.V. Parizotto, R.F. Fernandez, C.M.P. Marques, J.M.C. Bueno, Stud. Surf. Sci. Catal. 167 (2007) 421–426.
[12] H. Jeong, K.I. Kim, D. Ki, I.K. Song, J. Mol. Catal. A Chem. 246 (2006) 43–48.
[13] J.S. Chang, S.E. Park, H. Chon, Appl. Catal. A: Gen. 145 (1996) 111–124.
[14] W.D. Zhang, B.S. Liu, C. Zhu, Y.L. Tian, Appl. Catal. A: Gen. 292 (2005) 138–143.
[15] H. Inoue, N. Hatanaka, K. Kidena, S. Murata, M. Nomura, J. Jpn. Pet. Inst. 45 (2002) 314–320.
[16] J.-S. Chang, S.-E. Park, J.W. Yoo, J.-N. Park, J. Catal. 195 (2000) 1–11.
[17] M. Inaba, K. Murata, M. Saito, I. Takahara, N. Mimura, Reac. Kinet. Catal. Lett. 77 (2002) 109–115.
[18] J.M. Ginsburg, J. Pina, T. El Solh, H.I. de Lasa, Ind. Eng. Chem. Res. 44 (2005) 4846–4854.
[19] W. Nimwattanakul, A. Luengnaruemitchai, S. Jitkarnka, Int. J. Hydrogen Energy 31 (2006) 93–100.
[20] A. Kaengsilai, A. Luengnaruemitchai, S. Jitkarnka, S. Wongkasemjit, J. Power Sources 165 (2007) 347–352.
[21] S. Tosiri, M.S. Thesis, The Petroleum and Petrochemical College, Chulalongkorn University, Bangkok, Thailand, 2005.
[22] F.E. Trigueiro, D.F.J. Monteiro, F.M.Z. Zotin, E. Falabella Sousa-Aguiar, J. Alloys Compd. 344 (2002) 337–341.
[23] Y.S. Khodakov, I.D. Mikheikin, V.S. Nakhshunov, V.A. Shvets, V.B. Kazanskii, K.M. Minachev, Russ. Chem. Bull. 18 (1969) 465–470.
[24] D. Kiessling, K. Hagenan, G. Wendt, A. Barth, R. Schoellner, React. Kinet. Catal. Lett. 39 (1989) 89–93.
[25] M. Afzal, G. Yasmeen, M. Saleem, J. Afzal, J. Therm. Anal. Cal. 62 (2000) 277–284.
[26] Z. Hou, O. Yokota, T. Tanaka, T. Yashima, Appl. Catal. A: Gen. 253 (2003) 381–387.
[27] C.-W. Hu, J. Yao, H.-Q. Yang, Y. Chen, A.-M. Tian, J. Catal. 166 (1997) 1–7.
[28] P. Cañizares, A. de Lucas, F. Dorado, D. Pérez, Appl. Catal. A: Gen. 190 (2000) 233–239.
[29] A.M. Diskin, R.H. Cunningham, R.M. Ormerod, Catal. Today 46 (1998) 147–154.
[30] J.S. Feeley, W.M.H. Sachtler, Catal. Lett. 9 (1991) 377–386.
[31] M. Suzuki, K. Tsutsumi, H. Takahashi, Y.S. Suzuki, Zeolites 9 (1989) 98–103.
[32] S. Wang, G.Q. Lu, Energy Fuels 10 (1996) 896–904.
[33] J.R. Rostrup-Nielsen, Catalysis: Science and Technology, Springer, 1984.
[34] Z.L. Zhang, X.E. Verykios, Catal. Today 21 (1994) 589–595.
[35] J.B. Wang, S.-Z. Hsiao, T.-J. Huang, Appl. Catal. A: Gen. 246 (2003) 197–211.
[36] D. Halliche, O. Cherifi, A. Auroux, Thermochim. Acta 434 (2005) 125–131.